ARCHIVES OF ACOUSTICS
20, 2, 151–169(1995)

GENERATION AND DETECTION OF ACOUSTIC WAVES IN MICROWAVE CAVITIES

M. ALEKSIEJUK AND W. PAJEWSKI

Laboratory of Acoustoelectronic
Institute of Fundamental Technological Research
Polish Academy of Sciences
(00–049 Warszawa, Świętokrzyska 21)

This paper containes a detailed analysis of the conditions of acoustic wave excitation in retrant-type, microwave cavities, obtained by means of the methods field. Dependence of the resonance frequency on the resonator parameters and the material constants of a piezoelectric sample placed in the resonator is given. Construction of the resonators investigated and the experimental data concerning their parameters in the 0.210 GHz frequency range are presented. Results of attenuation measurements of waves in lithium niobate and bismuth-germanium oxide crystals obtained by applying the resonators described are also shown.

1. Introduction

Present ultrasonic technology and physics need acoustic sources with higher frequencies. Piezoelectric plate transducers traditionally used for the ultrasound generation become useless, first — from technological reasons (breaking of thin plates), and moreover troublesome because efficiency of transformation of the electric energy into the acoustic one (for harmonic frequencies) is low (losses are proportional to the square of frequency). Therofore, at the end of the fifties BARAŃSKI [1] and BÖMMEL and DRANSFLED [2, 3] proposed the method of existing the acoustic wave in a piezoelectric rod (quartz), one end of which was placed in a microwave resonator. Detection of the generated acoustic waves was done by the Bragg-type light diffraction measurement. Those methods were applied in solid body investigations at frequencies of 0.3–3 GHz. Investigations of the liquids were initiated by LEZHNEV [4]. Measurements in a higher frequency range were also made [5, 6]. In this paper the results of investigations, which represent an extension of the above mentioned method, togehter with a precise analysis of generation and detection conditions of hypersonic waves in the gigacycle frequency range, are presented. Dependence of the resonance frequency on the cavity parameters is determined. The resonators and the measurement setup made in IFTR for acoustic measurements in the gigacycle frequency range are described.

2. Excitation of hypersonic vibrations in resonator cavity

Generation of hypersounds by means of a cavity consists in the non-resonance surface layer excitation of vibrations of a pizoelectric rod, which is placed in a strong electric field of a microwave resonator. The excited hypersonic pulse on the surface layer of this rod, propagates as a consequence of the piezoelectric effect, along the rod, is reflected and returns to the origin of this rod. As a result of the inverse piezoelectric effect, it produces a new electromagnetic pulse, recorded by a microwave detection setup. In the rod with low acoustic losses, this pulse can be reflected many times and produces the subsequent echoes (Fig. 1).

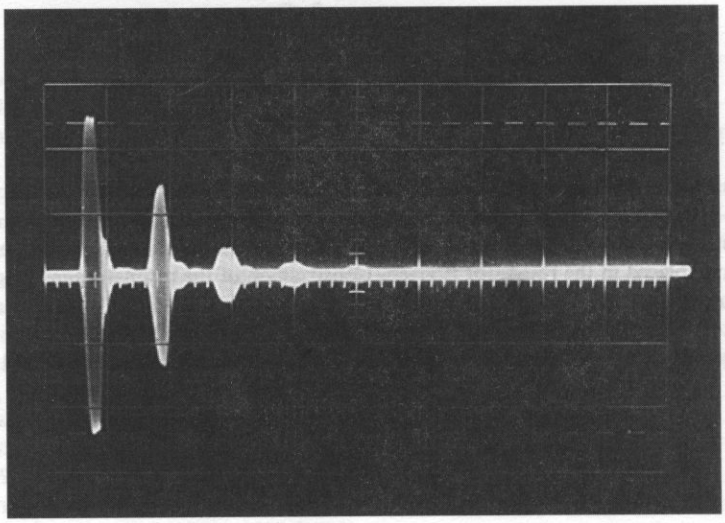

Fig.1. Sequence of electric echoes produced in the resonator as a result of repeated reflections of the hypersonic pulse in piezoelectric rod (frequency 600 MHz, room temperature).

In order to describe the generation phenomenon more precisely, the following assumptions are made: the piezoelectric rod is X-out, the one surfaces of it is placed at $x_1=0$, and the hypersonic wave propagates along the x_1 — axis of the rod (Fig. 2)

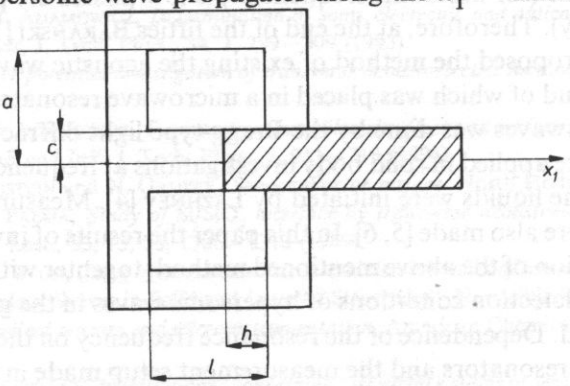

Fig.2. Parameters of the coaxial resonator.

A high-frequency electric filed $E_1(t)$ is also applied in this direction. In quartz with the density ρ, the mechanical stress σ_1 is determined by the expression:

$$\sigma_1 = c_{11}\varepsilon_1 - e_{11}E_1(t), \tag{2.1}$$

where c_{11} and e_n are the elasticity and piezoelectric constants, respectivelly, and ε_1 is the relative deformation. The equation for the displaced is obtained from the equation of motion

$$\rho = \frac{\partial^2 u_1}{\partial t^2} = \frac{\partial \sigma_1}{\partial x_1} = e_{11}\frac{\partial \varepsilon_1}{\partial x_1} - \frac{\partial}{\partial x_1}(e_{11}E_1), \tag{2.2}$$

or

$$\frac{\partial^2 u_1}{\partial x_1^2} = \frac{1}{V_t^2}\frac{\partial^2 u_1}{\partial t^2} = \frac{\partial}{\partial x_1}\left(\frac{e_{11}}{c_{11}}E_1\right), \tag{2.3}$$

where $(c_{11}/\rho)^{1/2}$ is the velocity of lingitudional wave propagation along x-axis the quartz. From Eq. (2.3) one can see that gradient of the electric field is the source of hypersonic waves. This gradient is large only on the surface of the piezoelectric rod, because inside the rod the electric filed gradully decreases with the distance.

Supposing the solutions of that equation to have the harmonic form:

$$E_1 = E_1^0 e^{-i\omega t}, \quad u_1 = u_1^0 e^{-i\omega t}, \tag{2.4}$$

Eq. (2.3) becomes

$$\frac{\partial^2 u}{\partial x_1^2} + k^2 u_1^0 = \frac{\partial}{\partial x_1}\left(\frac{e_{11}}{c_{11}}E_1^0\right), \tag{2.5}$$

where $k^2 = \varepsilon^2/v_1^2$.
Since the Green functions

$$G(x_1.x_1') = i/2k \exp(\mathrm{ik} \mid x\text{-}x' \mid) \tag{2.6}$$

are the solution of a homogenous equation

$$\partial^2 G/\partial x_1^2 + k^2 G + \delta(x_1 - x_1) \tag{2.7}$$

one can obtain

$$u_1^0(x_1) = \int \frac{l}{2k} \exp\left(ik \mid x_1 - x_1' \mid \frac{\partial}{\partial x_1'}\left(\frac{e_{11}}{c_{11}}E_1^0\right)\right) dx_1. \tag{2.8}$$

The largest spatial changes of the electric field occur at the boundary, therefore one can approximate the term corresponding to the source by a δ — function. The vaves which propagate in the x — direction are reflected from the free boundary. The boundary condition can be fulfilled by introducing the second apparent source at

$x_1 = x_0$, and by extending the rod to infinity. Next, two sources are transformed to a single one by passing to the limit for $x_0 = 0$. This gives

$$u_1^0(x_1) = \lim_{x_0 \to 0} \frac{iE_1^0 c_{11}}{2kc_{11}} \int \exp(ik \mid x_1 - x_1' \mid \delta(x_1' - x_0) + \delta(x_i + x_o)] dx_1' = \frac{iE_i^0 e_{11}}{kc_{11}} \exp(ikx_1) \tag{2.9}$$

for $x > 0$

Since the displacement is a real quantity, one takes only the real part of this expression,

$$u_1 = \frac{e_{11} E_1^0}{kc_{11}} \sin(\omega t - kx_1). \tag{2.10}$$

Now it is possible to find the acoustic energy flux and the efficiency of transformation. The density of the acoustic energy R in the rod equals

$$R = 1/2 \; c_{11} (\varepsilon_1^0)^2. \tag{2.11}$$

This energy propagates with velocity v_1 from the surface A. According to (2.10), the deformation equals

$$\varepsilon_1 = \frac{\partial u_1}{\partial x_1} = -\frac{e_{11}}{c_{11}} E_1^0 \cos(\omega t - kx_1), \tag{2.12}$$

and consequently, the amplitude of deformation is equal to $e_{11} E_1^0 / c_{11}$. In this case, the acoustic power obtained is given by

$$S = 1/2 \; e_{11}^2 (E_1^0) A v_l / c_{11}. \tag{2.13}$$

To determine the efficiency coefficient, this power must be compared with the electric power P deliveerd to the cavity. This power equals

$$P = \frac{\omega}{Q} 1/2 \; \varkappa \; (E_1^0) V, \tag{2.14}$$

where Q, V and $\varkappa$ are the quality factor of the resonator, its volume and the dielectric permeability of the rod, respectively.
Then

$$S/P = \frac{e_{11}^2}{\varkappa c_{11}} \frac{A v_l Q}{\omega V} = k_{11}^2 \, A v_l / \omega V, \tag{2.15}$$

where $k_{11} = (e_{11}^2 / \varkappa c_{11})^{1/2}$ is the electromechanical coupling coefficient.

The resonance frequency of the resonator, presented in literature [7], is described by following formula:

$$f_r = \frac{c'}{2\pi}\left[\frac{\varepsilon l c^2}{2h}\, lg\,(a/c)\right]^{-1/2} \tag{2.16}$$

where c' is the light velocity and ε is the dielectric constant. The dependence of frequency f_r, on the resonator parameters, calculated from this formula, is shown in Fig. 3. The dependence was obtained on the assumption that the piezoelectric rod was in contact with the resonator pivot. The case of a gap between the rod and pivot was examined by CARR [8] and, for different resonator shapes, by FUISAVA[9]. However, the theoretical results obtained by them did not coincide with the experiments in a satisfactory manner. Furthermore, our experimental investigations showed that in some cases, particulary the case of samples with large dielectric constants, it was not possible to tune the cavity resonator up. Different unexpected effects were observed which made it imposible to tune the resonator described below indicates the reasons for these difficulties and enables us to make the resonator possess the required features.

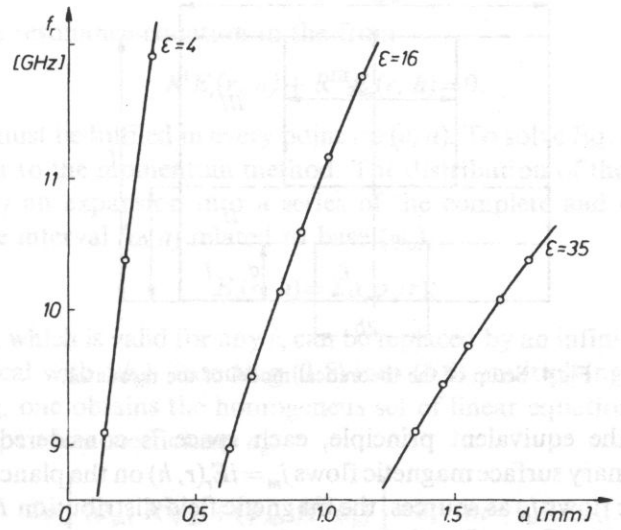

Fig.3. Resonance frequencies for the resonator with parameters 2a=11 mm, 2b=2.5 mm and l=3 mm, calculated from Eq. (16).

The Eq. (2.16) was obtained by means of the circuit methods. Namely, the resonator has been described as a set consisting of both an inductance created by the short section of the concentric line, and a capacitance between the central line and the internal surface of the resonator. The coaxial resonator described is the so-called capacitance shortened resonator [10, 11]. This resonator is made from an ordinary resonator by forming an air gap in the inner line of the resonator. In this manner, a new space with a homogeneus electric field is created and that produces the additional capacitance.

Introduction of the dielectric sample with a high value of the dielectric constant (for instance lithium niobate) to the describe by the circuit methods. Another difficulty in applying these method is due to fact that the part of the resonator in which the sample is placed, has not a strictly capacitive character, because in this space the magnetic filed energy is also accumulated. In particular the value of permeability of the sample, it is possible to obtain the resonance at the distance which corresponds to the depth of the sample immersed in the resonator in the considered space. The field distrribution in this resonator is, of course, unfavourable for the excitation of the hypersonic wave in the sample. These considerations concern the case when the resonance frequency in constant. This case corresponds to the situation in our experiment, when the magnetron generator (from radar emitter) is applied. For these reasons, it is necessary to use the methods for the description of the resonator in our configuration.

In this case the resonance state is obtained in the following manner [11, 12]:

a) The inside of the resonator is divied into space by planes (Fig. 4), in which the Helmholtz solution can be found analytically.

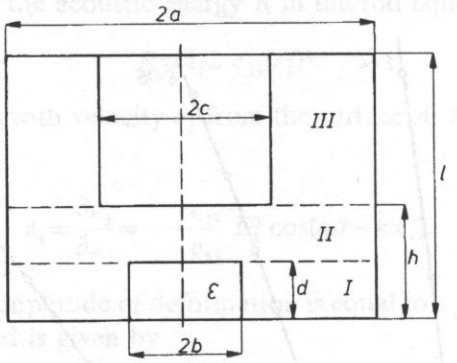

Fig.4. Setup of the theoretical model of the resonator.

b) Appyling the equivalent principle, each space is considered separately by introducing imaginary surface magnetic flows $j_m = iE_r(r, h)$ on the planes of separation.

c) Treating the flows j_m as sources, the magnetic field distribution H in the divided space is found by the Green function method.

d) Imposing the condition of continuity of the field H on the separation boundaries, the resonance condition is found in the form of the equation, which combines the resonance frequency with the material parameters of the sample and the dimensions of the resonator.

3. Model of an ideal resonator and parameters of the real one

First, according to the aformetioned procedure, one considers the particular case $h=d$, i.e. the situation when the dielectric contacts with the central line of the resonator. This case has an accurate solution.

The resonance condition has the form of a condition of continuity on the boundary $z=h$

$$H^{\mathrm{I}}(r, H)—H^{000}(r, h)=0, \tag{3.1}$$

where the magnetic fields in all spaces are expressed by the flows j_m and the proper Green functions

$$\begin{aligned} H^{\mathrm{I}}(r, z)&=i\omega\varepsilon\int G^{\mathrm{I}}(r, r', z, h)E_r(r', h)dr', \\ H^{\mathrm{III}}(r, z)&=—i\omega\varepsilon\int G^{\mathrm{III}}(r, r', z, h)E_r(r', h)dr. \end{aligned} \tag{3.2}$$

Functions G^{I} and G^{III} can be found by the methods described by FRIEDMAN [12] and JAWORSKI [13].

Introducing the symbol of integral operator

$$R_{\Psi}(r, h)=i\omega\varepsilon\int G(r, r', z, h)\Psi(r', h)dr, \tag{3.3}$$

one obtains the resonance equation in the from

$$R^{\mathrm{I}}E_r(r, h)+R^{\mathrm{III}}E_r(r, h)=0, \tag{3.4}$$

This equation must be fulfiled in every point $r\in(c, a)$. To solve Eq. (3.4), one uses the methods similar to the momentum method. The distribution of the field $E_r(r, h)$ can be expressed by an expansion into a series of the complete and orthogonal set of functions in the interval (c, a) related to base (φ_n),

$$E_r(r, h)=\Sigma a_n\varphi_n(r). \tag{3.5}$$

Next, Eq. (3.4), which is valid for any r, can be replaced by an infinite series, where φ_n is a base identical with $\{\psi_n\}$. Inserting (3.5) into (3.4), multiplying the results by ψ_n and integrating, one obtains the homogeneus set of linear equations with respect to the unknow expansion coefficients a_n:

$$\Sigma a_n\left[(\psi_m, R^{\mathrm{I}}\varphi_n)+(\psi_m, R^{\mathrm{III}}\varphi_n)\right]=0, \quad m=0,1,2,3,... \tag{3.6}$$

where $(\psi, R\varphi)$ denotes the scalar product $\int\psi R\varphi\ \mathrm{d}r$.

The set of equations (3.7) has a solution, when its characteristic determinant equals zero.

$$\det\left\{(\psi_m, R^{\mathrm{I}}\varphi_n)+\psi_m, R^{\mathrm{III}}\varphi_n\right\}=0. \tag{3.7}$$

Since both base sets, $\{\varphi_n\}$ and $\{\psi_m\}$, are infinite, the exact solution can be only obtained as a limiting case when $m, n\to\infty$. In practice, finite values $m, n\leqslant M$ are assumed but the approximate solution converges to the exact one when M is assumed to be sufficiently large. First of all, the rate of convergence to the exact solution depends on the choice the base functions φ_m and ψ_m. It will assumed below that

$$\varphi_0=\psi_0=1/ln(a/c)r, \quad n=0;$$
$$\varphi_n=\psi_n=Z_1(\alpha_n r) \,\|\, N \,\| \quad n=1,2,3..., \tag{3.8}$$

where N denotes the normalization factor, α_n are the subsequent solutions of the equation $Z_0(\alpha_n c)=0$, nad I_p and N_n denote the Bessel and Neumann functions of order p respectively. Set $\{\varphi_n\}=\{\varphi_m\}$ is complete and orthonormal with r in the interval (c, a).

It appears that function $\varphi_0=\psi_0=1/\ln(a, c)r$ reproduces quite well the distribution of the field $E_r(r, h)$ and, due to that, further calculations may be confined to the zero-order approximation of Eq. (3.7). Inserting φ_0, ψ_0 to (3.7) and integrating, one obtains the equation for the resonance frequency in the from:

$$\frac{1}{k\,\mathrm{tg}\,k(l-h)}+\frac{1}{k\,\mathrm{tg}\,(kh)}-\frac{\pi}{2h\ln(a/c)}$$
$$\sum_{n=0}^{\infty}\frac{\left[vbJ_1(ub)Z_0(vb)-\dfrac{ub}{\varepsilon}J_0(ub)Z_1(vb)Z_0(vc)\right]}{v^2\left[vbJ_1(ub)Z_0(vb)-\dfrac{ub}{\varepsilon}J_0(ub)J_1(vb)\right]}=0, \tag{3.9}$$

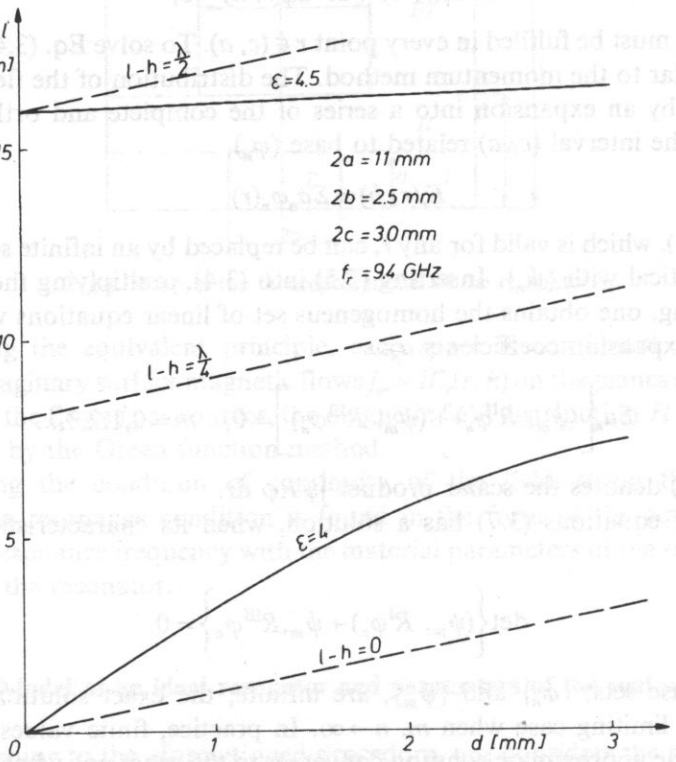

Fig.5. Dependence of the resonator length on the heigth of the piezoelectric rod from parameters 2a=11 mm, 2b=2.5 mm, 2c=3.0 mm, f=9.4 GHz.

where:

$$Z_p(vr)=N(vc)J_p(vr)-J(vc)N_p(vr), \quad p=1,2,$$

$u^2=k^2-(n\pi/h)^2$
$v=k^2-(n\pi/h)^2, \quad n=0,1,2,...,$
$k=2\pi/\lambda$

u denotes the so-called Hankel coefficient: $u=1$ 1 for $n=0$, and $u=2$, for $n=1,2,...$.

If u^2 or v^2 have negative values, then the function J_p and N_p must be replaced by the modified Bessel functions. Examples of the results of calculations for $\varepsilon_w=4$ and $\varepsilon_w=45$ are presented in Fig. 5. These calculation were carried out to determine l as a function of h for the following parameters: $a=5.5$ mm, $b=1.25$ mm, $c=1.5$ mm, $f_r=9.4$ GHz. It should be noticed that for $\varepsilon_w=45$ the lenght of the coaxial part of the resonator is $\lambda/4<1-h<\lambda/2$. This means that space l lies above the self-resonance and has an inducative character. As it has been mentioned before, this effect indicates that the space l can be replaced by a supplementary capacitance. This means that the circuit methods are useless in the description of such resonators.

Generalization of the applied method to the case of three spaces, i.e. $h>d$ (Fig. 4), is connected with considerable calculation difficulties. One of the possible methods of solution of this problem is based on the assumption of two unknown distributions of the field $E_r(r)$ on the boundaries $z=d$ and $z=h$, calculation of the field H_φ in a manner similar to that described above, and next, on the introduction of two conditions of continuity at the boundaries of the spaces. As a results, one obtains a double set of linear equations with respect to the unkown coefficients of the expansion of fields $E_r(r, d)$ and $E_r(r, h)$ into the series of phase functions. As before, vanishing of the characteristic determinant of the set of equations is the resonance conditions. Application of this method gives potentially very accurate results, but it requires the solution of a large set of equations. Confining the considerations to the zero-order approximation, we observe that the results, in the limiting case $d=h$, lead to errors larger then before. Another possibility is to treat the space I and II toghether and adjust the solutions is to the boundary $z=h$. This approch is simpler because it consist in adjusting the solutions in two, not three, spaces. However, it decreases the accuracy of the analysis.

In such a case the aproximate resonance equation has the following form:

$$1/[k\,\mathrm{tg}\,k(l-h)]+A/(k_{10}^2-k^2)+B=0. \tag{3.10}$$

At the zero approximation the coefficients A and B can be considered as constants. They can be determined from two resonance states, $d=0$ and $d=h$, calculated by means of the described method. In turn, k_{10}^2 can be calculated by an analysis of the homogeneus space $I+II$ or estimated by interpelation between the resonance frequencies of the space $I+II$, calculated $d=0$ and $d=h$. In Fig. 6 some results of calculations of k_{10} are presented, corresponnding to the linear interpolation and the case when $d<h$. The calculations were carried out for $\varepsilon_w=4$ and $\varepsilon_w=45$ to determine

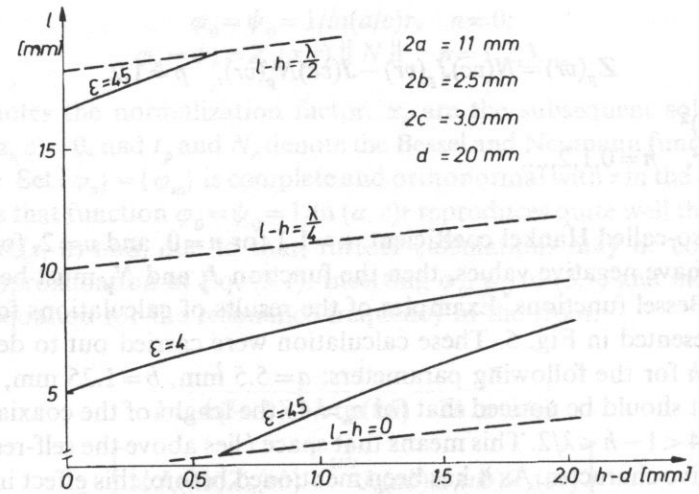

Fig.6. Dependence of the resonator length on the width of the gap.

l as a function of the width of the air gap $(h-p)$, other parameters being constant: $a=5.5$ mm, $b=1.25$ mm, $c=1.5$ mm, $d=2$ mm, $f_r=9.4$ GHz. For $\varepsilon_w=4$ one can observe the monotonic dependence of l on $(h-d)$. When the width of the gap increase, then the resultant capacitance of the space $I+II$ decreases, and so the length of the coaxial part $(l=h)$ increase. The dependence for $\varepsilon_w=45$ is more interesting when the space $I+II$ is of an inductive character for a small width of the gap and, as in the previous case, the length of coaxial part lies in the range $\lambda/4<l-h<\lambda/2$. For $h-d=0.6$ the selft-resonance of the space $I-II$ is obtained. It corresponds to the short-circuit in the plane $z=h$ i.e. $l-h=0$ or $l-h=\lambda/2$. Further increase of the gap width leads to the situation similar to the case $\varepsilon_w=4$, i.e. the space $I+II$ is of a capacitive character and the length of the coaxial part lies in the range $0<l-h<\lambda/4$.

Comparison of the results of the presented above with experimental data necessitates to account for the following facts:

- the resonator presented in Fig.2 is an idealized model of the real system, in which many simplifying assumptions have been made,
- in the nature of things, the method of calculation applied is an approximate one.

In what follows, these two factors will be discused. One of the fundamental simplifications consists in the assumption that the resonator has no hole in the place, where the dielectric sample should be put. Thus the sample is placed directly on the bottom of the resonator. This simplification resulted from numerical estimation of the lowest frequency of propagation of cylindrical modes in the dielectric sample with the largest assumed permeability $\varepsilon_w=45$.These calculations indicated that the resonance frequency was higher than the assumed 9.4 GHz, at which the resonator would be excited. Consequently, the cylindrical modes would be attenuated in the dielectric very quickly and the microwave energy would not be emitted outside the

resonator. For this reason it could be expected that the error caused by the existence of a hole in the real resonator would not have any significant influence on the value of the calculated resonance frequency. The experimental measurements have supported this assumption. Changes of the resonance frequency were unnoticeable after elimination of the hole. Influence of the hole on the quality factor of that resonator is more difficult to estimate, because the depth of the penetration depends on the sample.

The analyzed resonator is a system which is lossless and isolated from surroudings, but in the reality the system is coupled with the surroundings and energy losses occur in the walls and the dielectric material. The influence of the elements, which are coupled with the wave-guide line, is difficult to estimate. It is known, however, that this influence on the resonance frequency can be neglected when coupling with the wave-guide is sufficiently small.

The effect of radiation into surroundings from the dielectric rod, transmitted through the hole placed in the bottom of the resonator, is easier to estimate. With the assumptions that the diameter of the rod is equal to 2.5 mm and the frequency $f_r = 9.4$ GHz, this rod becomes a section of the subcritical wave-guide, fulfilled by the dielectric and excited in the TM_{01} type. For instance, the depth of penetration of the electromagnetic field energy along the rod axis is approximately equal to 0.35 mm for $\varepsilon_w = 45$. This means that the field energy, which is accumulated inside the rod below the bottom of the resonator, can be neglected, and replacement of the hole in the resonator bottom by a plane of perfect conductivity is possible for the values of d and h assumed in these considerations.

In relation to the energy losses and the corresponding finite quality factor the losses in the walls and in the coupling elements are small under typical conditions, and they can be estimated by measurements of the quality factor of the resonator without the sample. On the other hand, the energy losses in the piezoelectric sample depend on the dielectric and acoustic (attenuation) parameters and its volume. The calculations have been made under the assumption of a losseless (real) dielectric, but the calculation formulas are vaild also for a complex one. In particular, it is possible to assume that the energy lost in the dielectric depends approximately on the dimension d, the other dimensions of the resonator being fixed. As a result, the quality factor of the resonator is, approximately, inversely proportional to the height of the sample, d and a reasonable compromise is needed between the requirements of effective coupling of the electromagnetic field with the sample (large d), and the large quality factor of the system (small d)

Estimation of the quality of the investigated resonator by means of numerical methods is extremely complicated and it could not be done with a sufficient accuracy. Thus, the measurements of this factor were carried out experimentally for several samples. From these measurements it follows that this factor is not very large and is of the order of several hundred. Moreover, the quality factor depends at least on two factors, which are difficult to control. They are: uncertain contact in the inner line of

the resonator at the entrance to the resonator cavity, and the position of the coupling antenna inside the resonator. Significant differences in the quality factor measurements were observed even for small displacements of these elements. In the case when the measurements were performed in a stable range, the dependence of the quality factor and the resonance frequency upon the position of the samples and the position of the microwave short-circuit element are similar to those presented in Fig.7 and 8.

Independently of that, the calculations performed are of an approximate character.

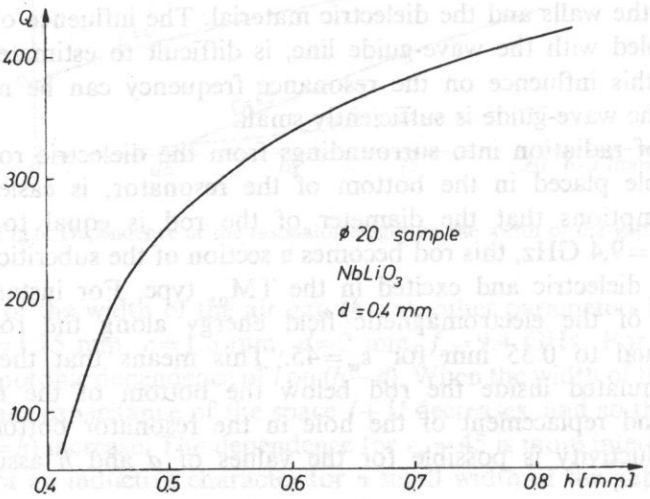

Fig.7. Dependence of the quality factor of the resonator on the inner line position.

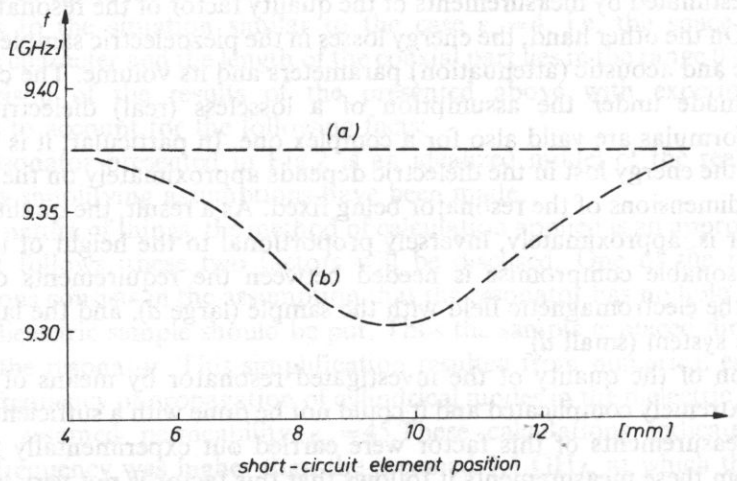

Fig.8. Dependence of the resonance frequency on the position of the microwave short-circuit element (from experiments) a) subcritical coupling b) supercritical coupling.

Typical starting data have been assumed to estimate the dimensions of the construction.

The results of calculations concerning the influence of the sample position and of the gap $h-d$ on the resonator length, are shown in Fig.9 and 10. The discontinuity of the resonator length l is of particular interest for $\varepsilon_w=40$. One can notice that only for the sample with $\varepsilon_w=3.38$ (quartz) it is posible to get the contact of the sample with the

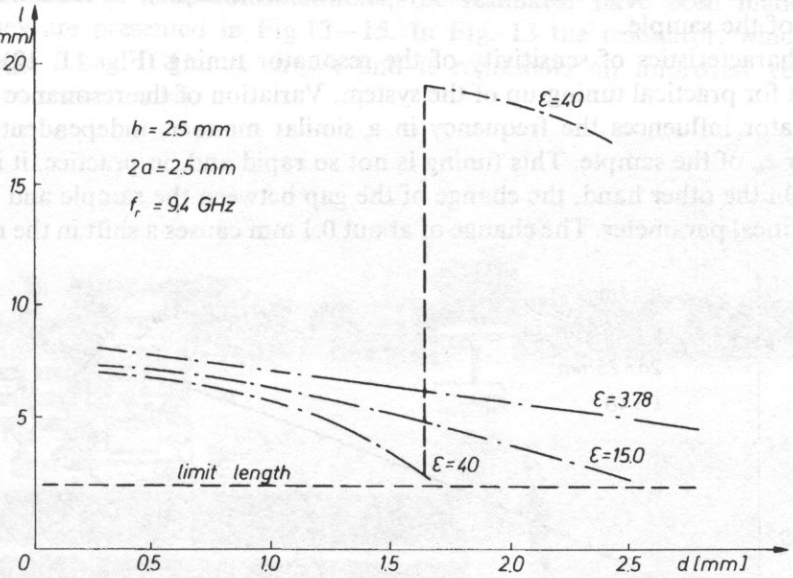

Fig.9. Dependence of the resonator length on the position of the sample.

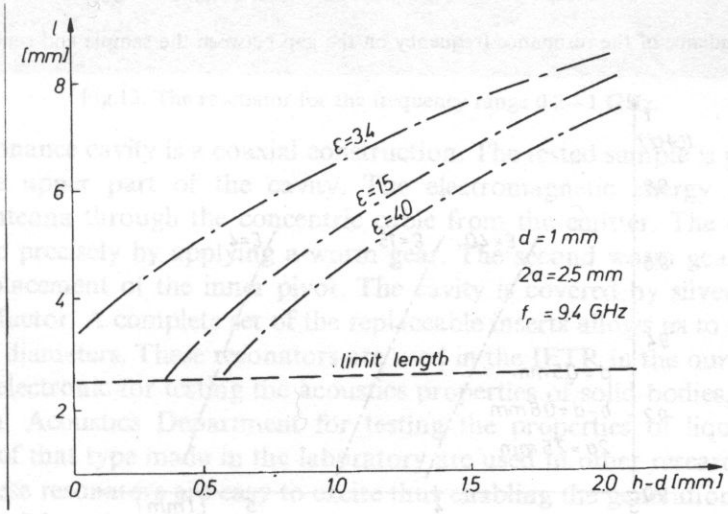

Fig.10. Dependence of the resonator length on the gap between the sample and central line.

inner line of the resonator. For $\varepsilon_w = 15$ and 40 it cannot be done in a continuous manner because of a step change of the resonance length. In both the figures dashed lines mark the actual resonator length of about 2.5 mm. This length from the existence of the exciting antenna in the real resonator. One of the ways to shif the limit, at which the step change of the resonator length occurs, towards smaller values of $h-d$ (this gives, practically, the possibility of getting the tuning continuity in the range of small gaps between the inner line and the sample), is reduction of the diameter of the sample.

The characteristics of sensitivity of the resonator tuning (Figs.11, 12) are very important for practical tuning-up of the system. Variation of the resonance length of the resonator influences the frequency in a similar manner, independently of the parameter ε_w of the sample. This tuning is not so rapid and, in practice, it is easy to control. On the other hand, the change of the gap between the sample and the inner line is a critical parameter. The change of about 0.1 mm causes a shift in the resonator

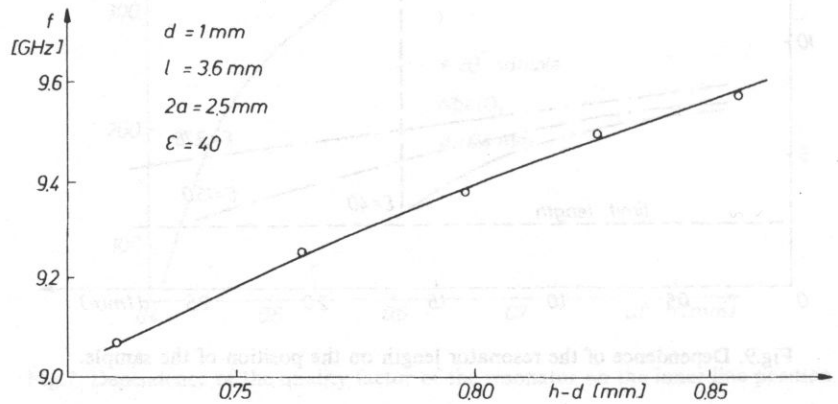

Fig.11. Dependence of the resonance frequency on the gap between the sample and central line.

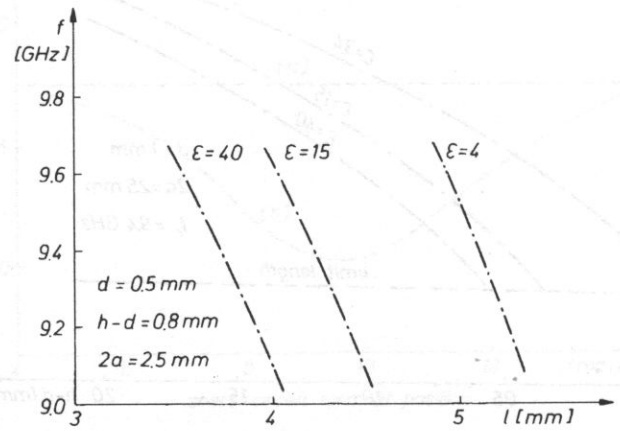

Fig.12. Dependence of the resonance frequency on the resonance length for different samples.

tuning-up frequency by about 500 MHz. For this reason, the micrometric screw was used in the resonator model to displace the inner line.

4. Results of measurements

On the basis of such considerations, the resonator have been made in the IFTR. They are presented in Fig.13–15. In Fig. 13 the resonator, which works in the range 0.2–1 GHz; is shown and it represents an improved version of the LEZHNEV resonator [4].

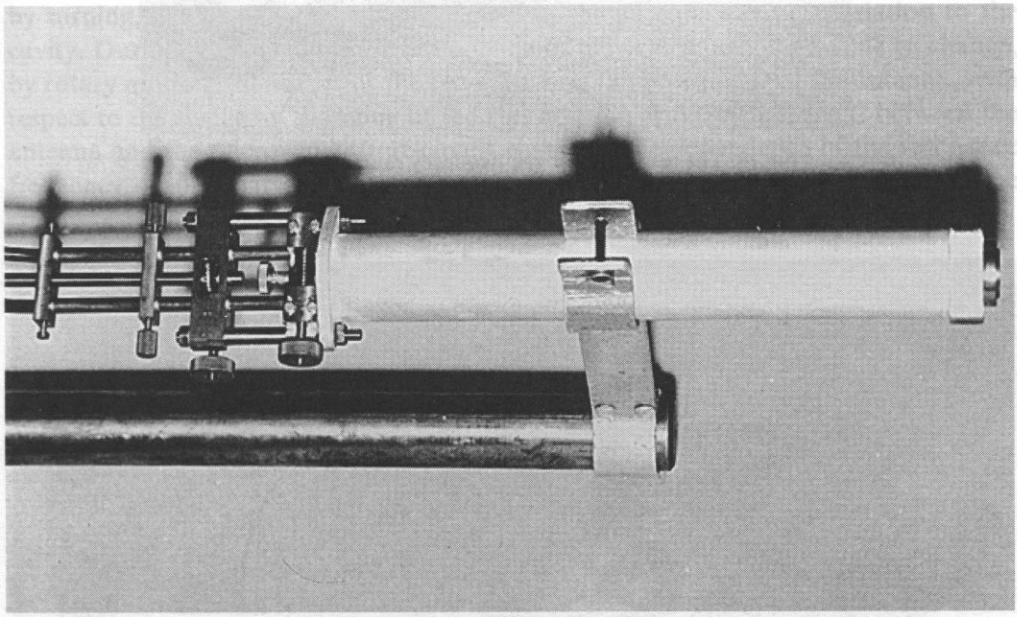

Fig.13. The resonator for the frequency range 0.2–1 GHz.

The resonance cavity is a coaxial construction. The tested sample is placed in the hole in the upper part of the cavity. The electromagnetic energy supplies the coupling antenna through the concentric cable from the emitter. The cavity could be tuned up precisely by applying a worm gear. The second worm gear is used for precise displacement of the inner pivot. The cavity is covered by silver to increase the quality factor. A complete set of the replaceable inserts allows us to test the rods of different diameters. These resonators are used in the IFTR in the our Laboratory of Acoustoelectronic for testing the acoustics properties of solid bodies, and also in the Physical Acoustics Department for testing the properties of liquids. Several resonators of that type made in the laboratory are used in other research centers in Poland. These resonators are easy to excite thus enabling the generation of acoustic waves. The „Matec" setup is especially suitable for cooperation with such resonators.

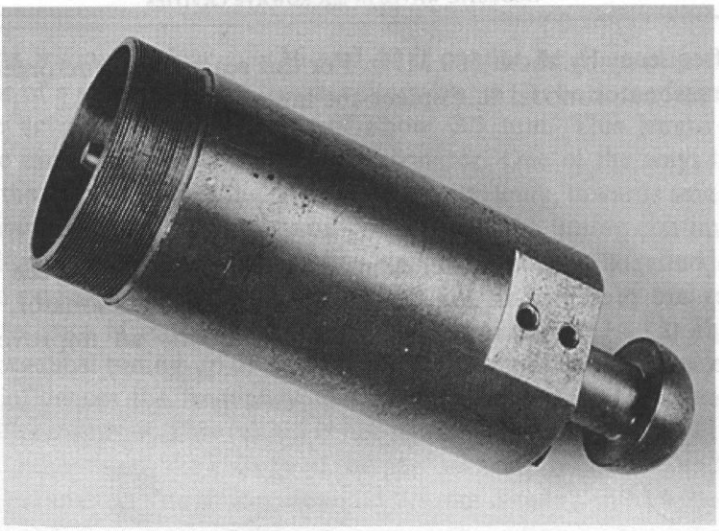

Fig.14. The resonator for the frequency range 3–4 GHz.

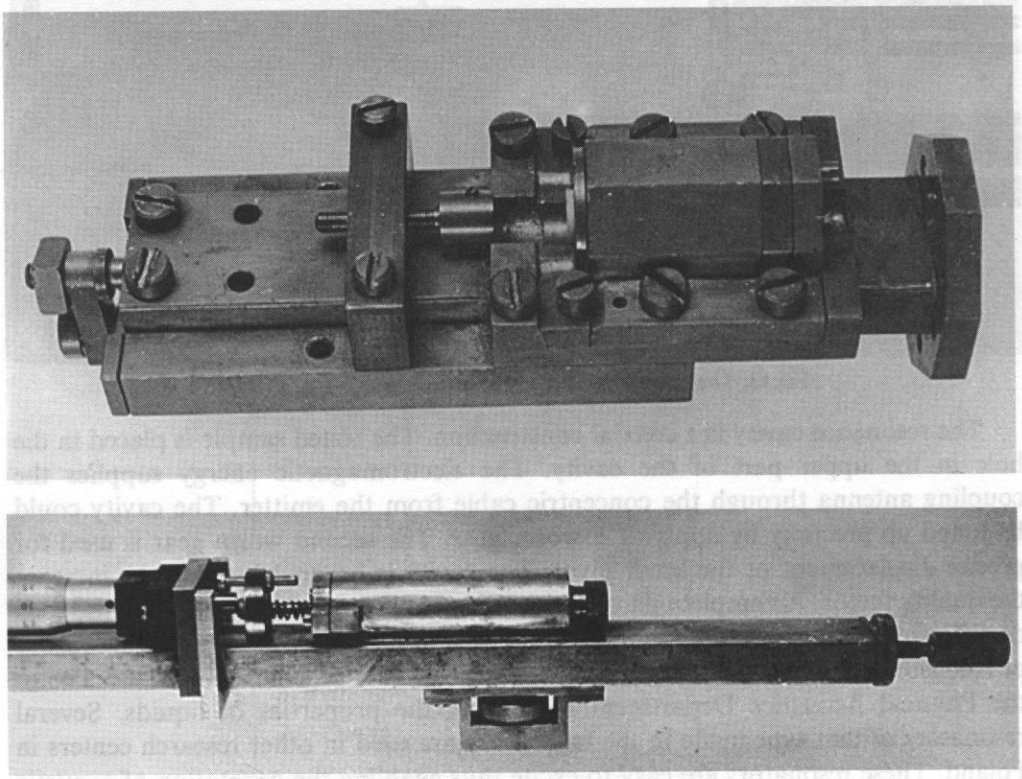

Fig.15. The resonator for the frequency range 9–11 GHz.

The resonator, presented in Fig.14, works in the 3–4 GHz frequency range. Those presented in Fig.15 were made in the IFTR for the 9–11 GHz frequency range. One of them has the displeceable diaphragm *a*, and the second one — an inner pivot which can be displaced by the micrometer screw *b*. These resonators were used in the setup made in the IFTR [14].

Construction of the cavity resonator is schematically presented in Fig.16. The resonator connected to the section of the wave-guide with the microwave short-circuit element (*3*). Copuling of the cavity with the wave-guide occurs by the antenna (*2*). The cavity is tuned by means of the pivot (*5*), attached to the diaphragm (*4*). The piezoelectric rod (*1*) is inserted into the cavity. In the course of tuning one can change, by turning, the piezoelectric rod plunge L in the antenna cavity in relation to the cavity. During the experiment, from outside of the cryostat, it is possible to change, by rotary motion, the values of the plunge L and the position D of the antenna, with respect to the cavity by changing of the rod position and the distance C between the antenna and the microwave short-circuit element. The dependence of the resonance frequency of the cavity on the parameters C, D, and L has been estabilished in the course of experiments.

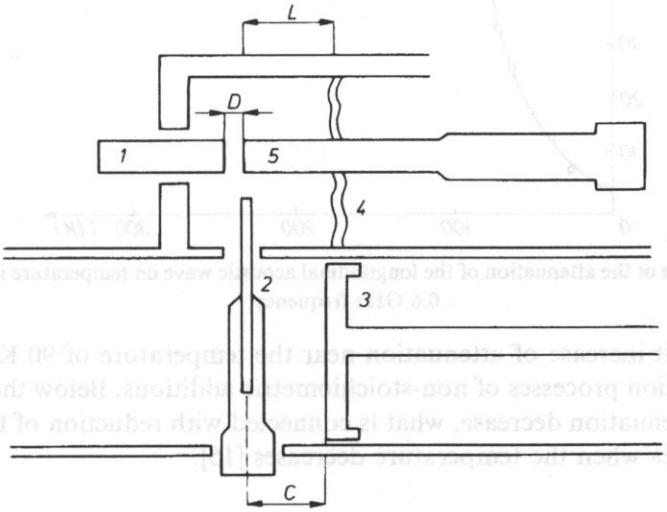

Fig.16. Construction of the reentrant type cavity. *1*-piezoelectric rod, *2*-antenna, *3*-microwave short-circuit element, *4*-diaphragm, *5*-pivot.

In Fig.17 and 18 the results of measurements of the acoustic wave attenuation in crystal, performed by means of the above described resonators, are presented. These measurements were made at cryogenic temperature. The variation of attenuation for the bismuth-germanium oxide (Bi_{19} GeO_{20}) in the 100 direction and the lithium niobate ($NbLiO_3$) crystals, are shown in Fig. 17 and 18, respectively. In the former dependence (Fig.17) one can notice two ranges of temperature, above and below 100 K. In the former one the attenuation of acoustic wave is connected with scattering of the wave on thermic phonones.

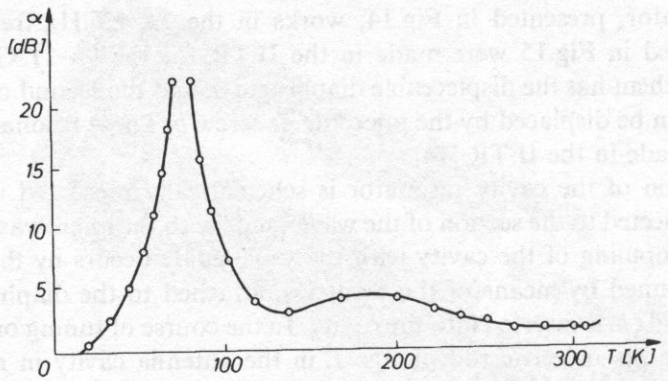

Fig.17. Dependence of the attenuation of the longitudinal acoustic wave on temperature in $Bi_{19}GeO_{20}$ crystal at 0.6 GHz frequency.

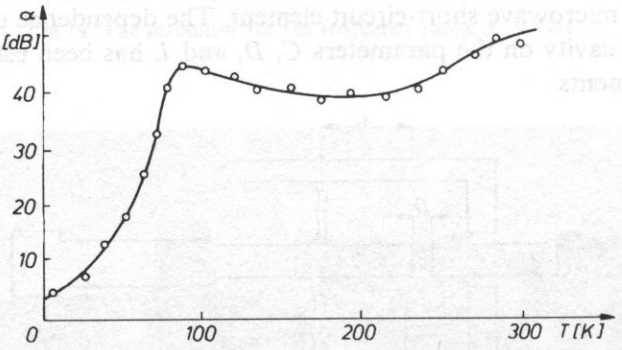

Fig.18. Dependence of the attenuation of the longitudinal acoustic wave on temperature in $NbLiO_3$ crystal 0.6 GHz frequency.

A significant increase of attenuation near the temperature of 90 K is connected with the relaxation processes of non-stoichiometric additions. Below the temperature of 50 K the attenuation decrease, what is connected with reduction of the amount of termic phonones when the temperature decreases [15].

References

[1] K.N. Barański, Kristalografia, 2, 299 (1957).
[2] H.E. Bömmel and K. Dransfeld, Phys. Rev. Lett., 1, 234 (1958).
[3] H.E. Bommel and K. Dransfled, Phys. Rev. Lett., 2, 249 (1959).
[4] N.B. Lezhnev, *Hypersonic methods of investigations in physics of liquide state*, (in Russian), IFTR PAS, Warsaw 1978.
[5] J. Ilukor and E.H. Jacobsen, Science, **153**, 1113 (1966).
[6] J. Ilukor and E.H. Jacobsen, in: Physical acoustics [Ed.] W.P. Mason 1974, vol. VI, ch. 4, p. 1910.
[7] J.W. Tucker and V.W. Rampton, *Microwave ultrasonic in solid state physics*, 1972, Ch. 3, p. 90.
[8] P.H. Carr, J. Acoust. Soc. Am., **41**, 75 (1967).

[9] K. FUISAWA, IRE Trans. MIT, **6** 10 (1958).
[10] T. MORAWSKI, W. GLOGIER and T. MODELSKI, Report of Warsaw University of Technology (in Polish) 330 (1988).
[11] A. MILEWSKI, *Methods of material testing in the range of very high frequencies* (in Polish), WKŁ Warsaw 1983.
[12] B. FREIDMAN, *Principles and techniques of applied mathematics*, New York 1956.
[13] A. JAWORSKI, IEEE Trans. MTT, **26**, 256 (1978).
[14] M. ALEKSIEJUK, Scientific Instrument 1990.
[15] M. ALEKSIEJUK and I. MALECKI, *Electronic and acoustic methods of material testing*, (in Polish), Warsaw 1984. p. 581.